Inorganica Chimica Acta 399 (2013) 166–171

Contents lists available at SciVerse ScienceDirect

Inorganica Chimica Acta

journal homepage: www.elsevier.com/locate/ica

An oxorhenium(V) Schiff-base complex: Synthesis, characterisation, structure, spectroscopic and electrochemical aspects

Smita Majumder [a], Arnab Bhattacharya [a], Jnan Prakash Naskar [b], Partha Mitra [c], Shubhamoy Chowdhury [a,*]

[a] *Department of Chemistry, Tripura University, Suryamaninagar, Tripura 799 022, India*
[b] *Department of Chemistry, Inorganic Chemistry Section, Jadavpur University, Jadavpur, Kolkata 700 032, India*
[c] *Department of Inorganic Chemistry, Indian Association for the Cultivation of Science, Jadavpur, Kolkata 700 032, India*

ARTICLE INFO

Article history:
Received 5 October 2012
Received in revised form 18 December 2012
Accepted 20 January 2013
Available online 30 January 2013

Keywords:
Oxorhenium(V) complex
Schiff-base ligand
Fluorescence
Electrochemistry
DFT calculation

ABSTRACT

Reaction of equimolar proportion of *trans*-$ReOCl_3(PPh_3)_2$ with HL, a 1:1 Schiff-base condensate of salicylaldehyde and allylamine, in chloroform gives rise to $ReO(L)(PPh_3)Cl_2$ **1a** in optimal yield. **1a** has been characterized by C, H and N microanalyses, ESI-MS, FT-IR, UV–Vis spectra, molar conductivity measurements. The X-ray crystal structure of **1a** reveals that it is an octahedral *cis-Cl,Cl* oxorhenium(V) complex. The rhenium center is in 'NO_2Cl_2P' coordination sphere. **1a** crystallizes in the orthorhombic space group $Pna2_1$ with $a = 17.3541(11)$, $b = 10.2737(6)$, $c = 15.2113(10)$ Å, $V = 2712.0(3)$ Å^3 and $Z = 4$. The photophysical and electrochemical aspects of **1a** have been studied. Electrochemical studies in dichloromethane show Re(V) to Re(VI) oxidation at 1.437 V along with a reduction of Re(V) to Re(IV) at −0.705 V versus Ag/AgCl. Excitation of **1a** in chloroform at 460 nm leads to a fluorescent emission at 525 nm with a quantum yield (Φ) of 0.17. Geometry optimization of the *cis-Cl,Cl* complex **1a** vis-à-vis its *trans* analogue, *trans-Cl,Cl* complex **1b**, have been performed at the level of the density functional theory (DFT). It is revealed that **1b** is more stable than **1a** by 4 kcal per mole of energy in gas phase.

1. Introduction

The chemistry of rhenium has been studied extensively. The obvious purposes are manifold. The potential application of $^{186/188}$Re radioisotopes in nuclear medicine is an important thrust area [1]. Technetium has no stable isotope [2]. Due to similarity in physical and chemical properties between rhenium and technetium [3], the rhenium compounds often serve as synthetic models for the mimicry of the widely used ^{99m}Tc in the field of radiopharmaceuticals. Development of diagnostic imaging agents based on technetium/rhenium is an ever-stretching and renewed area of research. One of the successful attempts along that line is based on the syntheses of Schiff-base ligands to stabilize the $[MO]^{+3}$ core for M = Tc(V) and Re(V) [4]. The reason is obvious. Schiff-base ligands offer a considerable degree of versatility in terms of their substituents, coordination flexibility, varied range of denticity and geometry. Thus there exists distinct possibility for designing technetium and rhenium complexes with desired biological properties employing tailor-made Schiff-base ligands [1]. Again, the chemistry of rhenium involves several oxidation states ranging from –I to VII. In particular, the oxidation of Re(V) complexes to Re(VII) complexes is an essential step in the catalytic cycle by which such a redox couple catalyzes oxygen atom transfer (OAT) reaction [3]. One of the most versatile and highly efficient transition metal catalysts known to date is methyltrioxorhenium(VII) and some oxorhenium(V) complexes were found to be highly successful in OAT reactions [3].

Another area of investigations on rhenium compounds is their application as white organic light-emitting devices (WOLEDs) which are connected with their unique electrochemical, photophysical and photochemical properties. The most frequently studied compounds of this type are complexes containing the $[Re(CO)_3]^+$, *trans* $[ReO_2]^+$ and $[ReO]^{3+}$ cores [5].

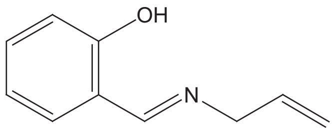

HL

In this context 2-allyliminomethyl-phenol (HL), a Schiff-base ligand, seems to be promising. This ligand can adopt chelating as well as bridging modes of binding to metal centers in bidentate anionic (L^{1-}) form. Earlier L^{1-} has been employed to stabilize a good number of metal ions like Cu(II), Zn(II), Pd(II) and Sn(IV) [6]. Curi-

---

* Corresponding author.
E-mail address: shubha103@yahoo.com (S. Chowdhury).

0020-1693/$ - see front matter © 2013 Elsevier B.V. All rights reserved.
http://dx.doi.org/10.1016/j.ica.2013.01.018

ously there is no such report with rhenium. This aspect of rhenium chemistry has kindled our interest to work on the oxorhenium(V) core particularly with HL. Herein we wish to report the preliminary outcome of our endeavor along that line – synthesis, characterization, structural elucidation, fluorescence and redox behavior of a novel oxorhenium(V) complex of HL for the first time. Calculations at the level of density functional theory (DFT) were also performed to corroborate the structural and spectral observations.

2. Experimental

2.1. Materials and physical measurements

Ammonium perrhenate (Sigma–Aldrich Chemicals) was used as received. The precursor, *trans* [$ReOCl_3(PPh_3)_2$] was prepared and characterized following the method of Chatt and Rowe [7]. Allylamine hydrochloride and salicylaldehyde were procured from Sigma–Aldrich and were used without any further purification. Microanalyses were performed with a Perkin–Elmer 2400II elemental analyzer. FT-IR spectra in solid phase were recorded as KBr pellets with a Perkin–Elmer FTIR-100 spectrophotometer. UV–Vis absorption spectra of the ligand, HL as well as the complex, **1a** were recorded on a Perkin–Elmer Lambda 25 spectrophotometer. Solution conductivity measurements were carried out in DMF solution of **1a** at room temperature on a Systronics (India) direct reading conductivity meter (model 304). Electrospray Ionization Mass Spectra (ESI-MS) in the positive ionization mode were recorded on a Waters Qtof Micro YA263 spectrometer. Electrochemical experiments were performed on a BAS Epsilon electrochemical workstation (Model CV-50) under nitrogen in dry and degassed dichloromethane at 293 K. The supporting electrolyte was tetra-*n*-butylammonium perchlorate (TBAP) (0.1 M). The conventional three-electrode assembly was comprised of a Glassy Carbon (GC) working electrode, a platinum wire counter electrode and a Ag/AgCl reference electrode. All potentials reported herein are referenced to Ag/AgCl. Emission spectrum was recorded with a Shimadzu RF-5000 spectrofluorimeter at room temperature (298 K) in dichloromethane solution under degassed condition. The fluorescence quantum yield (Φ) of the complex was determined using phenanthrene as a Ref. [8]. The complex and the reference dye were excited at the same wavelength maintaining nearly equal absorbance and the emission spectra were recorded. The area of the emission spectrum was integrated and the quantum yield was calculated according to the following equation:

$$\Phi_S/\Phi_R = [A_S/A_R] \times [(\mathrm{Abs})_R/(\mathrm{Abs})_S] \times [\eta_S^2/\eta_R^2] \quad (1)$$

Here, Φ_S and Φ_R are the fluorescence quantum yields of the sample and the reference respectively. A_S and A_R are the area under the fluorescence spectra of the sample and the reference respectively; $(\mathrm{Abs})_S$ and $(\mathrm{Abs})_R$ are the respective optical densities of the sample and the reference solution at the wavelength of excitation; η_S and η_R respectively are the values of refractive indices for the sample and the reference.

2.2. Synthesis of ligand (HL)

The ligand (HL) was synthesized by mixing salicylaldehyde (5.33 mL, 50 mmol) and allylamine (3.66 mL, 50 mmol) in absence of any solvent. The resulting yellow reaction mixture was stirred for 6 h at room temperature. After stirring, the yellow liquid product so obtained was purified by distillation under reduced pressure. Yield: 5.63 g, 70%. *Anal.* Calc. for $C_{10}H_{11}NO$: C, 74.49; H, 6.88; N, 8.69. Found: C, 74.32; H, 6.68; N, 8.75%. FTIR (KBr, cm^{-1}): (O–H) 3492 (br, vs); (C=C) 1664 (m); (C=N) 1622 (vs). ^1H NMR ($CDCl_3$, 300 MHz) (, ppm): 8.33 (s, 1H, N=C*H*); 7.29 (t, *J* = 8.2 Hz, 1H, Ar); 7.22 (d, *J* = 7.6 Hz, 1H, Ar) 6.92 (d, *J* = 8.3 Hz, 1H, Ar); 6.80 (t, *J* = 7.5 Hz, 1H, Ar), 6.07–5.95 (ov m, 1H, C*H*=CH_2); 5.26 (d of d, *J* = 17, 1.3 Hz, 1H, CH = C*H*H); 5.17 (d of d, *J* = 10, 1.3 Hz 1H, CH=CH*H*) 4.25 (d, *J* = 5.5 Hz, 2H, C*H*$_2$CH=CH_2). (UV–Vis ($CHCl_3$), λ_{max} (ε, M^{-1} cm^{-1}): 244 (26 790); 345 (9 810). Mass spectra requires for the molecular ion peaks $C_{10}H_{11}ON$ 161.09, found 162.04 $[M+H]^+$, 184.11 $[M+Na]^+$.

2.3. Synthesis of [$ReO(L)PPh_3Cl_2$] (**1a**)

To a suspension of the *trans* $ReOC1_3(PPh_3)_2$ (0.416 g, 0.50 mmol) in chloroform (20 mL) was added ligand (HL) (0.081 g, 0.50 mmol) dissolved in 10 mL of chloroform drop wise with stirring. The resulting reaction mixture was heated under reflux for 3 h. During refluxing, the color changes from yellowish-green to green. The resulting solution was cooled to room temperature and was allowed to evaporate in the air to dryness to get a sticky green mass. This sticky green mass was washed thoroughly with diethyl ether to obtain a green powder. Yield: 292 mg 84%; *Anal.* Calc. for $C_{28}H_{25}Cl_2NO_2PRe$: C, 48.33; H, 3.62; N, 2.01. Found: C, 48.17; H, 3.71; N, 2.10%. FTIR (KBr, cm^{-1}): (C=C) 1664 (s); (C=N) 1610 (vs); (Re=O) 984 (vs); (Re–O) 687 (s). ^1H NMR ($CDCl_3$, 300 MHz) (δ, ppm): 7.66 (s, 1H, N=C*H*); 7.61–7.20 (ov m, 17H, 15H of PPh_3 and 2H of Ar); 6.95 (d, *J* = 8.3 Hz, 1H, Ar); 6.62 (d, *J* = 8.2 Hz, 1H, Ar); 6.25–6.10 (ov m, 1H, C*H*=CH_2), 5.27 (d of d, *J* = 17, 1.2 Hz 1H, CH=C*H*H); 5.18 (d of d, *J* = 10, 1.2 Hz, 1H, CH=CH*H*) 4.82 (d of d, *J* = 5.5, 4.2 Hz, 1H, C*H*HCH=CH_2); 3.84 (d of d, *J* = 5, 4.2 Hz, 1H, CH*H*CH=CH_2). UV–Vis (CH_2Cl_2), λ_{max} (ε, M^{-1} cm^{-1}): 245 (24 077); 358 (8 694); 410sh (2001); 460sh (730); 626 (80). Mass spectra requires for the molecular ion peaks $C_{28}H_{25}Cl_2NO_2PRe$ 695.37, found 696.14 $[M+H]^+$, 718.09 $[M+Na]^+$. Λ_M (DMF): Non-electrolyte.

2.4. X-ray crystal structure determination

Single crystals of the title complex, **1a** suitable for X-ray structure determination were selected from those obtained by slow direct diffusion of petroleum ether (40–60 °C) into a moderately concentrated solution of **1a** in dichloromethane at 298 K. An appropriate single crystal of **1a** was mounted on a Bruker SMART APEX II CCD area detector diffractometer at 298(2) K using graphite monochromatic Mo Kα radiation (= 0.71073 Å). Intensity data of **1a** were reduced using SAINT [9a] and the empirical absorption corrections were performed with SADABAS program [9b]. The structures of **1a** were solved by direct methods and refined by full-matrix least-square methods based on $|F|^2$ using SHELXL-97 [9c]. All non-hydrogen atoms were refined anisotropically. Hydrogen atoms were placed in calculated positions and constrained to ride on their parent atoms. Even the best single crystal employed for data collection, having been selected from the lot of **1a**, imparted diffused diffraction spots. This is indicative of a large mosaic spread. Some of the diffraction spots were overlapping. Consequently the integration of those spots could not be performed properly by the processing software. Thus a small portion of the collected reflections was excluded and the final structure was refined using the available data ($2.3 < \theta < 25.0°$). However, the reduced dataset was adequate to give rise a precise structure. All the calculations were carried out using SHELXS-97 [9c], SHELXL-97 and SHELXTL [9c] programs. The crystallographic data for the complex **1a** are summarized in Table 1.

2.5. Computational details

All computations were performed using the Gaussian03 (G03) [10a] software package. The Becke's three-parameter hybrid exchange functional and the Lee–Yang–Parr non-local correlation functional (B3LYP) [10b] were used throughout in this present

Table 1
Crystal data and structure refinement for **1a**.

Parameter	Complex **1a**
Formula	$C_{28}H_{25}Cl_2NO_2PRe$
Formula weight	695.57
Crystal system	orthorhombic
Space group	$Pna2_1$
Unit cell dimensions	
a (Å)	17.3541(11)
b (Å)	10.2737(6)
c (Å)	15.2113(10)
V (Å^3)	2712.0(3)
Z	4
T (K)	293
ρ_{calc} (g/cm^{-3})	1.704
μ (Mo Kα) (mm^{-1})	4.762
F(000)	1360
Crystal size (mm)	0.22 × 0.24 × 0.26
λ (Mo Kα) (Å)	0.71073
θ Ranges (°)	$2.3 < \theta < 25.0$
Total reflection	22644
Reflection independent (R_{int})	4760 (0.038)
h/*k*/*l*	−16, 20/−12, 12/−18, 18
Reflection observed ($I > 2\sigma$)	4222
R_1	0.0220
wR_2	0.0520
Goodness of fit (GOF) on F^2	1.04
Largest difference peak and hole (e Å^{-3})	0.67 and −0.37

$R_1 = \Sigma||F_o| - |F_c||/\Sigma|F_o|$, $wR_2 = [\Sigma w(F_o^2 - F_c^2)^2/\Sigma w(F_o^2)^2]^{1/2}$.
Calcd. $w = 1/[\sigma^2(F_o^2) + (0.\ 0166P)^2 + 0.5698P]$ where $P = (F_o^2 + 2F_c^2)/3$.

computation. Elements other than Re were assigned 6-31G(d) basis set in the course of calculation. For rhenium the Los Alamos effective core potential plus double zeta (LanL2DZ) [10c] basis set were employed. The geometric structures of the complexes in the ground state (S_0) were fully optimized at the B3LYP level. All the computed vibrational frequencies corroborate with the experimental vibrational spectrum of **1a** in terms of identical modes but with shifted positions**.** This is quite natural since our computations are only compatible in the gas phase. However, this can be regarded as a signature of the closeness of the two structures – one as determined by X-ray crystallography (minimum energy) *cis Cl*,*Cl* **1a** and the other, *trans Cl*,*Cl* **1b** as obtained from the course of geometry optimization process (global minimum energy structure). Thus there is a rationale between our experimental findings and our adapted theoretical computations at the DFT level.

3. Result and discussion

3.1. Syntheses

The ligand, HL, employed for the present work is a 1:1 Schiff-base condensate of allylamine and salicylaldehyde. The synthesis had been reported earlier [6a,11]. It seems from the earlier reports that the use of an organic solvent like methanol is crucial for the synthesis. Here for the first time we have generated it in a solvent-free condition. Thus our method is close to greenness. Subsequently we have attempted to explore the metal binding aspects of HL particularly with Re in its +V oxidation state. A novel oxorhenium(V) complex, $ReO(L)(PPh_3)Cl_2$ **1a** has been obtained out of the ligand exchange reaction in the course of our reaction of $ReO(PPh_3)_2Cl_3$ with the ligand (HL) in equimolar proportion in chloroform. The compound is stable in air, green in color and soluble in common organic solvents.

3.2. X-ray crystal structure

Green air-stable crystals of **1a** suitable for X-ray were obtained by slow direct diffusion of petroleum ether (40–60 °C) into a moderately concentrated solution of the compound **1a** in dichloromethane at room temperature. An ORTEP perspective view of the asymmetric unit along with the atom numbering scheme, is shown in Fig. 1. Selected metrical parameters are given in Table 2. The rhenium atom is at the center of a distorted octahedral environment. The basal plane is formed by the imino nitrogen of L$^-$, two chloride donor atoms and the phosphorous atom from PPh_3. The Re center is displaced by 0.125(2) Å towards Re=O from this basal plane. The monoanionic phenolate oxygen atom (O1) of the ligand is in *trans* position to the Re=O moiety. The occupancy of this *trans* position of O1 is justified in the spirit of the *trans* directing influence of the Re=O linkage on oxygen (here O1) from an axially bound ligand. This is the normal mode of binding of a salicylaldimine-derived ligand regardless of its denticity [12a,b,4e]. The Re1–O2 distance is 1.691(3) Å, a value typical for the oxorhenium(V) complex. The Re1–N1 distance is of 2.134(5) Å. This is within the stipulated range (2.11–2.32 Å) [11a–d] for a R–N single bond in oxorhenium(V) complexes. The O2–Re1–O1 angle is of 170.42(14)°. This value is in considerable deviation from the idealized value of 180° for a regular octahedral geometry. Thus the geometry around rhenium center in **1a** is distorted octahedral with a 'NO_2Cl_2P' coordination sphere of rhenium.

The majority of the known oxorhenium(V) complexes, $[ReOX_2(O\text{-}N)(PPh_3)]$ based on salicylaldimine based ligands display structures with halide ligands in *cis* relative dispositions [12c–g]. Our compound, **1a**, is not an exception. The Cl(1)–Re–Cl(2) angle is of 89.20(6)°, a value quite close to 90°. Thus **1a** is a *cis-Cl*,*Cl* complex with the Re–Cl bonds of 2.369(6) and 2.418(7) Å. This Re–Cl2 bond is *trans* to the Re–N(1) (imino-N of the ligand L$^-$) bond. A similar type of *trans* effect was observed earlier in oxorhenium(V) complexes [12].

3.3. Spectroscopic properties

3.3.1. FTIR and ^{1}H NMR spectroscopy

The Schiff-base ligand, HL shows a singlet at δ 8.33 ppm in its ^{1}H NMR spectrum owing to the presence of the imino-methine (–CH=N–) proton. The diagnostic C=N stretching band is found in its FT-IR spectrum at 1620 cm^{-1} [13]. Complex **1a** has been characterized by a number of physical methods including NMR spectroscopy. A significant upfield shift is observed for the imino-methine (–CH=N–) proton in the ^{1}H NMR spectrum of **1a**.

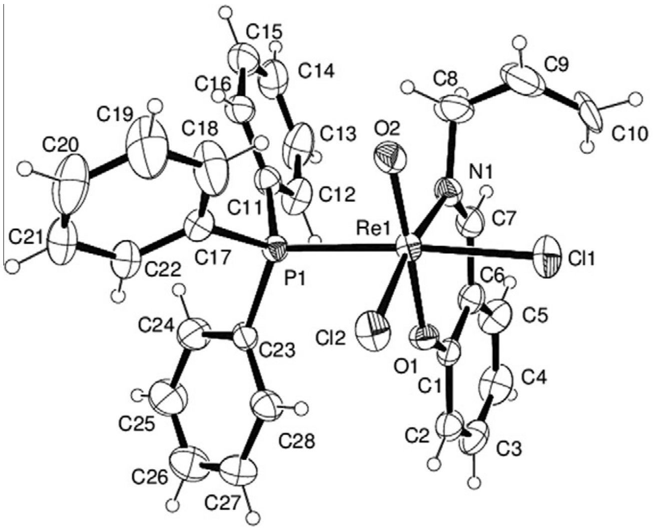

Fig. 1. ORTEP diagram of complex **1a** showing the atom labeling scheme with 30% probability ellipsoids.

Table 2
The selected experimental and optimized bond lengths (Å) and bond angles (°) for **1a**.

Bond lengths/bond angles	Experimental	Optimized
Re1–O1	1.930(3)	1.953
Re1–O2	1.691(3)	1.717
Re1–N1	2.134(5)	2.134
Re1–P1	2.462(6)	2.594
Re1–Cl1	2.418(7)	2.463
Re1–Cl2	2.369(6)	2.368
C9–C10	1.343(10)	1.349
Cl1–Re1–Cl2	89.20(6)	90.02
Cl1–Re1–N1	86.29(14)	85.81
Cl2–Re1–P1	90.02(4)	88.57
P1–Re1–N1	93.84(14)	94.94
O1–Re1–O2	170.42(14)	166.93
N1–C7–C6	128.0(5)	127.76
N1–C8–C9	110.5(5)	111.78

This is due to the binding of the ligand to the metal center. In our case the singlet resonance at δ 8.33 ppm for the free ligand, HL shifts to 7.66 ppm in its complex, **1a**. The methylene protons of the coordinated Schiff-base ligand appear at 4.82 ppm and 3.84 ppm. This difference in their chemical shift values can be explained in the spirit of molecular asymmetry in **1a**. The ligand, HL is coordinated in a plane parallel to the Re=O bond and there is distinct possibility of protons on methylene carbon experience different chemical environments due to the asymmetry of the molecule. The IR spectrum of the ReO(V) complex, **1a** exhibits a sharp band at 984 cm^{-1}, assignable to the characteristic stretching frequency of ν(Re=O) [12c–g].

The experimental vibrational spectrum of the *cis* complex, **1a** has been compared with the calculated (non-scaled) one in Fig. 2. The selected experimental and calculated IR frequencies of **1a** are tabulated in Table S1. The calculated vibrational stretches of the *cis* complex, **1a** are in good agreement with the experimental data. The experimental and the calculated IR spectra of the isomer, **1a** are almost similar in terms of their band positions, band intensity and shape of bands. It is pertinent to note that the calculated ν(Re–O) frequency value (642 cm^{-1}) for the complex **1a** is lower than its experimental value only by ~6%. However, this discrepancy is justified when seen from a theoretical perspective. Often the computed gas phase data are at variance with the experimental one. This is a natural consequence [14]. Moreover the calculated ν(Re=O) value was found to be exactly at the same magnitude as found by experiment (984 cm^{-1}).

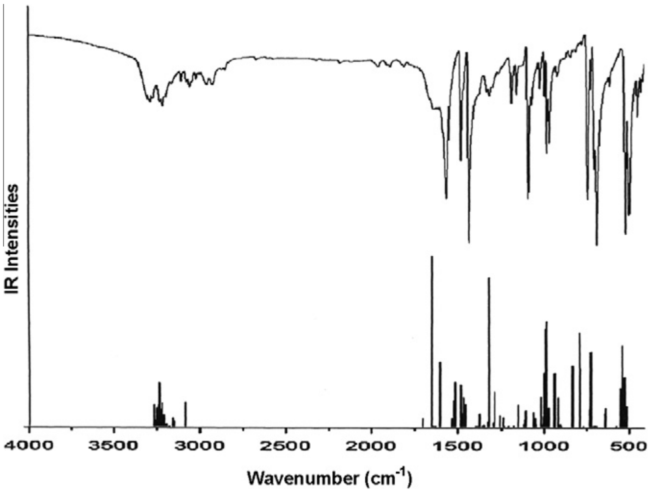

Fig. 2. The experimental (upper) and the calculated non-scaled (lower) vibrational spectra of complex **1a**.

3.3.2. UV–Vis absorption spectroscopy

The solution electronic spectrum (UV–Vis) of **1a** was recorded in chloroform and is shown in Fig. S1. The spectrum is characterized by strong absorption bands at 245 and 358 nm. The shapes and molar absorption coefficients of these high energy bands resemble the features of the free ligand, HL. Thus they can be assigned as the $\pi \rightarrow \pi^*$ transitions, centered mostly in the ligand (spin allowed $S_0 \rightarrow {}^1IL$ transition). The spectral position of the intraligand band at 358 nm is significantly red-shifted relative to the free ligand as a result of the coordination of the heavy metal core. Most likely this is due to the overlap of ligand to metal charge transfer (LMCT) transitions with intraligand transition band [15a]. With reference to earlier spectroscopic studies [16b,c], the weak shoulder at 410 nm is probably due to $(d_{xy})^2 \rightarrow (d_{xy})^1(d_{\pi}^*)^1$ $[{}^1A_1 \rightarrow {}^1B_2\ (a_2)^2 \rightarrow (a_2)^1(b_1)^1;\ {}^1A_1 \rightarrow {}^1B_1\ (a_2)^2 \rightarrow (a_2)^1(b_2)^1]$ transitions. A very weak shoulder (460 nm) and a band (626 nm) are likely due to the metal centered ${}^1A_1 \rightarrow {}^3B_2$ and ${}^1A_1 \rightarrow {}^3B_1$ spin forbidden transitions respectively.

3.3.3. Emission spectroscopy

The emission spectrum was recorded in the deaerated chloroform solution of **1a** at room temperature. This spectrum is shown in Fig. 3 **1a** exhibits fluorescence emission band centered at 525 nm upon excitation at 460 nm. The observed emission band is broad and shows no vibronic structure. In general the band position, multiplicity and the emission quantum yield are strongly dependent on the structure and its rigidity of the underlying complex. The fluorescence quantum yield (Φ) of **1a** is found to be 0.17. With reference to the previous spectroscopic work on this class of compounds [15b–f], the present emission in **1a** is originated most likely from $(d_{xy})^1(d_{xz})^1$ $[{}^3B_2]$ and $(d_{xy})^1(d_{yz})^1$ $[{}^3B_1]$ triplet excited states. Again in the excitation spectrum of **1a** monitored at 525 nm, broad bands at ca. 298 and 320 nm can also be deciphered. This spectral feature closely resembles the corresponding UV–Vis absorption spectrum. Thus it may be inferred that the ground state molecular structure of **1a** is retained in its excited state during excitation in chloroform.

3.4. Geometry optimizations

To elucidate the bonding properties of the *cis-Cl,Cl* **1a** and *trans-Cl,Cl* **1b,** calculations at the DFT level were undertaken. The geometries were optimized in singlet state using the DFT method with

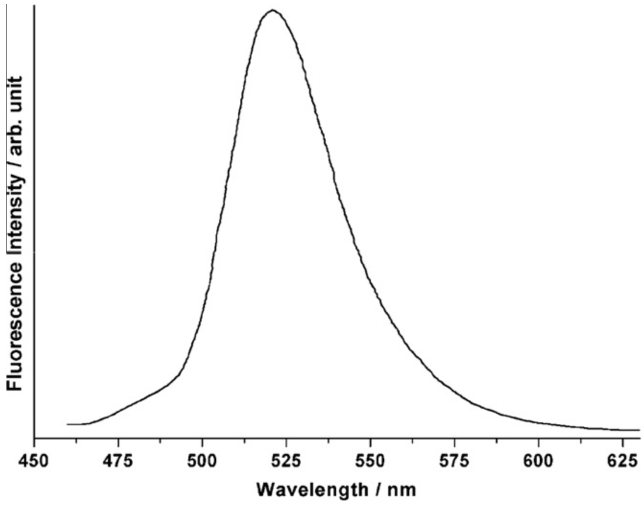

Fig. 3. The fluorescence spectrum of **1a** in chloroform obtained upon excitation at 460 nm.

the B3LYP functional. From the geometry optimization it was found

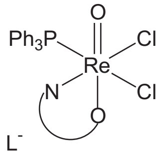

Cis Cl,Cl (**1a**)

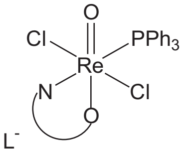

Trans Cl,Cl (**1b**)

that the *trans-Cl,Cl* **1b** isomer is more stable than the *cis-Cl,Cl* **1a** isomer by 4 kcal per mole of energy. However we have been able to isolate only the *cis-Cl,Cl* isomer, **1a** in solid state. In general, the predicted bond lengths and angles are in good agreement with the values obtained from X-ray crystallography. The largest discrepancy encountered was for the value of Re–P bond distance. This difference arises most likely either from the employed basis sets which were approximated to a certain degree or may due to the influence of the crystal packing on the values of the experimental bond lengths [14,16]. It is pertinent to note that the theoretical calculations do not consider the effects of chemical environment.

3.5. Electrochemistry

The electrochemical behavior of **1a** has been studied in dichloromethane by cyclic voltammetry at GC working electrode under a dry and degassed nitrogen atmosphere. The resulting cyclic voltammogram (CV) is shown in Fig. 4 and the peak potentials are tabulated in Table 3. On the positive side of the Ag/AgCl reference electrode, **1a**, exhibits one anodic wave (couple-I) with a peak potential of 1.531 V versus Ag/AgCl. The associated anodic peak current, i_{pa} is 12.36 A. The corresponding cathodic response is discernable in the subsequent back cycle with a peak potential value of 1.343 V versus Ag/AgCl and a concomitant cathodic peak current, i_{pc} of 9.83 A. The ligand, HL, is electrochemically dormant in the potential range of interest here. Thus this oxidation can safely be assigned as metal centered. Comparison of the voltammetric peak currents with those of the ferrocene-ferrocenium couple (0.442 V versus Ag/AgCl) under the same experimental condition establishes that the present oxidative response in **1a** involves one electron. So, the oxidation at +1.531 V versus Ag/AgCl corresponds to Re(V) to Re(VI) oxidation. The ratio of i_{pc} to i_{pa} is 0.80, a value near to unity. Again, i_{pc} increases with $v^{1/2}$ but not in proportionality. Proportional variation of i_p with $v^{1/2}$ is a genuine signature of the establishment of the Nernstian equilibrium of a redox couple at the electrode surface as predicted by Randles-Sevčik equation [17]. However, in our case the oxidative response is in clear deviation from this idealized equilibrium. Again, the cathodic peak in the reverse cycle is not totally absent. So the electrochemical event is not totally irreversible in nature. Thus this oxidative response is quasi-reversible in nature. This observed potential of the Re(VI)/Re(V) redox couple is comparable to the values reported earlier [16c,17].

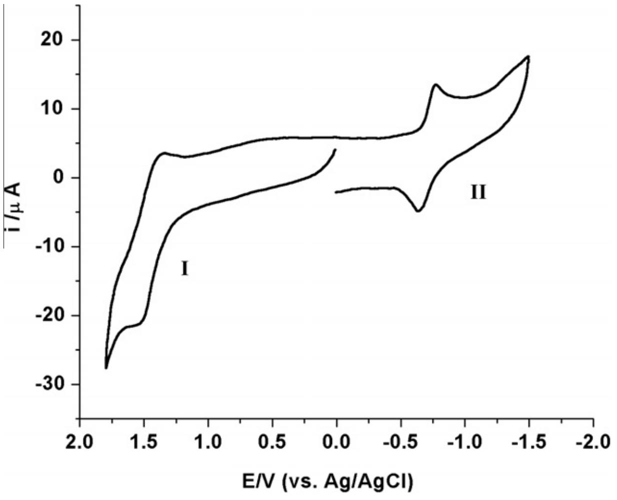

Fig. 4. CV of **1a** in dichloromethane at a scan rate of 100 mV s^{-1}. The analyte concentration was 0.97×10^{-3} M.

Table 3
Cyclic voltammetric data of compound **1a**.

Entry	E_{pa} (V)	E_{pc} (V)	ΔE (V)	$E^{\circ}_{1/2}$	i_{pc} (μA)	i_{pa} (μA)
Couple-I	1.531	1.343	0.188	1.437	9.83	12.36
Couple-II	−0.642	−0.768	0.126	−0.705	7.74	6.38

E_{pa} is the peak potential for the anodic wave, E_{pc} is the peak potential for the cathodic wave, $E_{1/2} = 1/2\,(E_{pa} + E_{pc})$, i_{pa} is the peak current for the anodic wave, i_{pc} is the peak current for the cathodic wave.

Our oxorhenium(V) complex again shows electrochemical response at $E_{1/2}$ value of −0.705 V (couple II) on the negative side of the Ag/AgCl electrode. Comparison of the voltammetric peak currents of the couple II with those of the ferrocene-ferrocenium couple (0.442 V versus Ag/AgCl) under the same experimental condition establishes that the present reductive event in **1a** involves one electron as earlier. Thus the above reductive response can be assigned as Re(V) to Re(IV) reduction. The cathodic peak current, i_{pc} of couple II is of 7.74 A. Subsequent anodic response in the reverse cycle can be discernable at −0.642 V versus Ag/AgCl with an anodic peak current, i_{pa} of only 6.38 A. The ratio of i_{pc} to i_{pa} is 1.21. This value is in considerable deviation from unity. The cathodic peak current, i_{pc}, increases with the square root of the scan rate ($v^{1/2}$), but not in proportionality. Again, the cathodic peak potential, E_{pc}, shifts more negatively with the increase in sweep rate, v. Based on these criteria, the metal centered reduction for **1a** at peak II is said to be quasi-reversible in nature [17]. Now it may be proposed that the following putative redox steps might be operative here:

$$[\mathrm{Re}^{VI}\mathrm{O(L)(PPh_3)Cl_2}]^+ + e^- \rightarrow [\mathrm{Re}^{V}\mathrm{O(L)(PPh_3)Cl_2}] \quad E_{1/2} = 1.437\mathrm{V}$$

$$[\mathrm{Re}^{V}\mathrm{O(L)(PPh_3)Cl_2}]^+ + e^- \rightarrow [\mathrm{Re}^{IV}\mathrm{O(L)(PPh_3)Cl_2}] \quad E_{1/2} = -0.705\mathrm{V}$$

The electrochemical reductions of oxo-Re(V) to Re(IV) with a one-electron transfer process has also been proposed in some of the previously reported oxorhenium(V) complexes. The reported mechanism [18] is akin to our present proposition.

4. Conclusion

Here we have synthesized and characterized a new oxorhenium(V) complex from a Schiff-base ligand, 2-allyliminomethylphenol (HL). The X-ray crystal structure of the complex, $[\mathrm{Re^{V}O(L)(PPh_3)Cl_2}]$ **1a**, reveals that the rhenium(V) center in **1a** is in distorted octahedral 'NO_2Cl_2P' coordination sphere. The two chloride donors are *cis* to each other. Thus **1a** can be described as a *cis-Cl,Cl* oxorhenium(V) complex. However, the DFT calculations at the gas phase reveal that the *trans-Cl,Cl* oxorhenium(V) complex, **1b** is more stable than **1a** by a magnitude of 4 kcal per mole. The ReO^{3+} complex also exhibits a blue luminescence upon excitation at its d–d absorption fold at 460 nm. The electrochemical studies of **1a** show Re(V) to Re(VI) oxidation along with a one electron reduction, Re(V) to Re(IV) in dichloromethane.

Acknowledgement

We wish to thank Dr. S. A. Hussain, Department of Physics, Tripura University for providing the workstation of GAUSSIAN 03W software for present computations. Financial support from the SERC under Department of Science and Technology (DST), India, is gratefully acknowledged. We solicit to bestow our gratitude to the reviewers for helping us in the course of its revision.

Appendix A. Supplementary material

CCDC 900491 contains the supplementary crystallographic data for this paper. These data can be obtained free of charge from The Cambridge Crystallographic Data Centre via www.ccdc.cam.ac.uk/data_request/cif. Supplementary data associated with this article can be found, in the online version, at http://dx.doi.org/10.1016/j.ica.2013.01.018.

References

[1] (a) W.T. Volkert, T.J. Hoffman, Chem. Rev. 99 (1999) 2269;
(b) J.R. Dilworth, S.J. Parrot, Chem. Soc. Rev. 27 (1998) 43;
(c) R. Schibli, P.A. Schubiger, Eur. J. Nucl. Med. Mol. Imaging 29 (2002) 1529.
[2] (a) G. Bandoli, M. Nicolini, U. Mazzi, F. Refosco, J. Chem. Soc., Dalton Trans. (1984) 2505;
(b) U. Mazzi, F. Refosco, F. Tisato, G. Bandoli, M. Nicolini, J. Chem. Soc., Dalton Trans. (1986) 1623;
(c) F. Tisato, F. Refosco, U. Mazzi, G. Bandoli, M. Nicolini, J. Chem. Soc., Dalton Trans. (1987) 1693;
(d) F. Refosco, F. Tisato, U. Mazzi, G. Bandoli, M. Nicolini, J. Chem. Soc., Dalton Trans. (1988) 611.
[3] (a) G.S. Owens, J. Arias, M.M. Abu-Omar, Catal. Today 55 (2000) 317;
(b) J.H. Espenson, Chem. Commun. (1999) 479;
(c) C.C. Romao, F.E. Kuhn, W.A. Herrmann, Chem. Rev. 97 (1997) 3197;
(d) J.H. Espenson, Coord. Chem. Rev. 249 (2005) 329.
[4] (a) A.R. Middleton, A.F. Masters, G. Wilkinson, J. Chem. Soc., Dalton Trans. (1979) 542;
(b) F.J. Femia, X. Chen, J.W. Babich, J. Zubieta, Inorg. Chim. Acta 300–302 (2000) 517;
(c) G. Du, P.E. Fanwick, M.M. Abu-Omar, Inorg. Chim. Acta 361 (2008) 3184;
(d) A. Sachse, N.C. Mösch-Zanetti, G. Lyashenko, J.W. Wielandt, K. Most, J. Magull, F. Dall'Antonia, A. Pal, R. Herbst-Irmer, Inorg. Chem. 46 (2007) 7129;
(e) M.V. Bẻreau, S.I. Khan, M.M. Abu-Omar, Inorg. Chem. 40 (2001) 6767.
[5] (a) F. Li, G. Cheng, Y. Zhao, J. Feng, S. Liua, Appl. Phys. Lett. 83 (2003) 4716;
(b) L.S. Hung, C.W. Tang, M.G. Mason, Appl. Phys. Lett. 70 (1997) 152.
[6] (a) N Poulter, M. Donaldson, G. Mulley, L. Duque, N. Waterfield, A.G. Shard, S. Spencer, A.T.A. Jenkins, A.L. Johnson, New J. Chem. 35 (2011) 1477;
(b) Y.-S. Uh, H. Zhang, C.M. Vogels, A. Decken, S.A. Westcott, Bull. Korean Chem. Soc. 25 (2004) 986;
(c) B.S. Saraswat, G. Srivastava, R.C. Mehrotra, J. Organomet. Chem. 129 (1977) 155.
[7] J. Chatt, G.A. Rowe, J. Chem. Soc. (1962) 4019.
[8] W.R. Dawson, M.W. Windsor, J. Phys. Chem. 72 (1968) 3251.
[9] (a) SAINT Plus, Data Reduction and Correction Program, v.6.01, Bruker AXS. Madison, Wisconsin, USA, 1998.;
(b) SADABAS v.2.01, Bruker/Siemens Area Detector Absorption Correction Program, Bruker AXS. Madison, Wisconsin, USA, 1998.;
(c) G.M. Sheldrick, Acta Crysallogr. Sect., A 64 (2008) 112.
[10] (a) M.J. Frisch, G.W. Trucks, H.B. Schlegel, G.E. Scuseria, M.A. Robb, J.R. Cheeseman, J.A. Montgomery, Jr., T. Vreven, K.N. Kudin, J.C. Burant, J.M. Millam, S.S. Iyengar, J. Tomasi, V. Barone, B. Mennucci, M. Cossi, G. Scalmani, N. Rega, G.A. Petersson, H. Nakatsuji, M. Hada, M. Ehara, K. Toyota, R. Fukuda, J. Hasegawa, M. Ishida, T. Nakajima, Y. Honda, O. Kitao, H. Nakai, M. Klene, X. Li, E. Knox, H.P. Hratchian, J.B. Cross, V. Bakken, C. Adamo, J. Jaramillo, R. Gomperts, R.E. Stratmann, O. Yazyev, A.J. Austin, R. Cammi, C. Pomelli, J.W. Ochterski, P.Y. Ayala, K. Morokuma, G.A. Voth, P. Salvador, J.J. Dannenberg, V.G. Zakrzewski, S. Dapprich, A.D. Daniels, M.C. Strain, O. Farkas, D.K. Malick, A.D. Rabuck, K. Raghavachari, J.B. Foresman, J.V. Ortiz, Q. Cui, A.G. Baboul, S. Clifford, J. Cioslowski, B.B. Stefanov, G. Liu, A. Liashenko, P. Piskorz, I. Komaromi, R.L. Martin, D.J. Fox, T. Keith, M.A. Al-Laham, C.Y. Peng, A. Nanayakkara, M. Challacombe, P.M. W. Gill, B. Johnson, W. Chen, M.W. Wong, C. Gonzalez, J.A. Pople, Gaussian, Inc., Wallingford, CT, 2004.;
(b) C. Lee, W. Yang, R.G. Parr, Phys. Rev. B 37 (1988) 785;
(c) P.J. Hay, W.R. Wadt, J. Chem. Phys. 82 (1985) 270.
[11] B. Erk, Y. Baran, Commun. Fac. Sci. Univ. Ank. Serie B 33 (1986) 27.
[12] (b) A. Sachse, N.C. Moˇsch-Zanetti, G. Lyashenko, J.W. Wielandt, K. Most, J. Magull, F.D. Antonia, A. Pal, R. Herbst-Irmer, Inorg. Chem. 46 (2007) 7129;
(b) T.I.A. Gerber, D. Luzipo, P. Mayer, Inorg. Chim. Acta 357 (2004) 429;
(c) J.M. Botha, K. Umakoshi, Y. Sasaki, Inorg. Chem. 37 (1998) 1609;
(d) Y. Miyashita, T. Ohashi, A. Imai, N. Amir, K. Fujisawa, K.-i. Okamoto, Sci. Technol. Adv. Mater. 6 (2005) 660;
(e) I.N. Booysen, T.I.A. Gerber, P. Mayer, Inorg. Chim. Acta 363 (2010) 1292;
(f) P. Traar, J.A. Schachner, L. Steiner, A. Sachse, M. Volpe, N.C. Mösch-Zanetti, Inorg. Chem. 50 (2011) 1983;
(g) A. Barandov, U. Abram, Polyhedron 28 (2009) 1155.
[13] K. Nakamoto, Infrared Spectra of Inorganic and Coordination Compounds, fourth ed., Wiley, New York, 1986.
[14] B. Machura, R. Kruszynski, J. Kusz, Polyhedron 27 (2008) 1679.
[15] (a) J.R. Lakowicz, Principles of Fluorescence Spectroscopy, third ed., Springer, Science, New York, 2006;
(b) V.W. W Yam, K.K. Tam, M.C. Cheng, S.M. Peng, Y. Wang, J. Chem. Soc., Dalton Trans. (1992) 1717;
(c) V.W. W Yam, Y.L. Pui, K.M.C. Wong, K.K. Cheung, Inorg. Chim. Acta 300–302 (2000) 721;
(d) G.A. Neyhart, K.J. Seward, J. Boaz, B.P. Sullivan, Inorg. Chem. 30 (1991) 4486;
(e) S. Sen, T. Mukherjee, S. Sarkar, S.K. Mukhopadhyay, P. Chattopadhyay, Analyst 136 (2011) 4839;
(f) J.S. Gancheff, R.Q. Albuquerque, A. Guerrero-Martinez, T. Pape, L.D. Cole, F.E. Hahn, Eur. J. Inorg. Chem. (2009) 4043.
[16] (a) B. Machura, M. Wolff, I. Gryca, Polyhedron 30 (2011) 142;
(b) T.I.A. Gerber, H.J. Kemp, J.G.H. Du Preez, J. Coord. Chem. 33 (1994) 171;
(c) B. Machura, M. Wolff, D. Tabak, Y. Ikeda, K. Hasegawa, Polyhedron 39 (2012) 76.
[17] R. Greef, R. Peat, L.M. Peter, D. Pletcher, J. Robinson, Instrumental Methods in Electrochemistry, Ellis Horwood Limited, England, 1985.
[18] (a) L.A. Bottomley, P.E. Wojciechowski, G.N. Holder, Inorg. Chim. Acta 255 (1997) 149;
(b) M. Pelecanou, I.C. Pirmettis, M.S. Papadopoulos, C.P. Raptopoulou, A. Terzis, E. Chiotelis, C.I. Stassinopoulou, Inorg. Chim. Acta 287 (1999) 142;
(c) D. Gambino, B.S. Parajón-Costa, H. Cerecetto, M. González, E. Kremer, E. Baran, J. Coord. Chem. 55 (2002) 1441;
(d) S. Chowdhury, M. Nogami, A. Canlier, N. Koshino, Y. Ikeda, Inorg. Chim. Acta 361 (2008) 1524;
(e) G.N. Holder, M.W. Kanning, Inorg. Chim. Acta 197 (1992) 67.